M. Tech (Computational Design)

STUDY OF EFFECTS OF INELASTICITY ON BUCKLING OF CYLINDRICAL SHELL UNDER AXIAL LOAD

A DISSERTATION

SUBMITTED IN PARTIAL FULFILLMENT OF THE REQUIREMENTS
FOR THE AWARD OF DEGREE
OF

MASTER OF TECHNOLOGY
IN
COMUTATIONAL DESIGN

Submitted by:

ISHITA

2K18/CDN/03

Under the supervision of

Dr. ATUL KUMAR AGARWAL
(Professor)

DEPARTMENT OF MECHANICAL & PRODUCTION ENGINEERING
DELHI TECHNOLOGICAL UNIVERSITY
(Formerly Delhi College of Engineering)
Bawana Road, Delhi-110042

JULY, 2020

ISHITA

2020

DEPARTMENT OF MECHANICAL AND PRODUCTION ENGINEERING

DELHI TECHNOLOGICAL UNIVERSITY

(Formerly Delhi College of Engineering)

Bawana Road, Delhi - 110042

CANDIDATE'S DECLARATION

I, Ishita, Roll No. 2K18/CDN/03, a student of M.Tech (Computational Design), hereby declare that the project Dissertation titled " **Study of Effects of Inelasticity on Buckling of Cylindrical Shell Under Axial Load** " which is submitted by me to the Department of Mechanical and Production Engineering, Delhi Technological University, Delhi in partial fulfillment of the requirement for the award of the degree of Master of Technology, is original and not copied from any source without proper citation**.** This work has not previously formed the basis for the award of and Degree, Diploma Associateship, Fellowship or other similar title or recognition**.**

Place: Delhi

Date: 31.8.2020

Ishita
2K18/CDN/03

DEPARTMENT OF MECHANICAL AND PRODUCTION ENGINEERING

DELHI TECHNOLOGICAL UNIVERSITY

(Formerly Delhi College of Engineering)

Bawana Road, Delhi – 110042

CERTIFICATE

I hereby certify that the Project Dissertation Titled **" Study of Effects of Inelasticity on Buckling of Cylindrical Shell Under Axial Load "** which is submitted by Ishita, 2K18/CDN/03 Department of Mechanical and Production Engineering, Delhi Technological University, Delhi in partial fulfillment of the requirement for the award of the degree of Master of Technology, is a record of the project work carried out by the students under my supervision. To the best of my knowledge this work has not been submitted in part or full for any Degree or Diploma to this University or elsewhere.

Place: Delhi
Date: 31.8.2020

Dr. Atul Kumar Agarwal
SUPERVISOR
(Professor)

ACKNOWLEDGEMENT

I would like to extend my gratitude to **Prof Vipin,** Head**,** Department of Mechanical And Production Engineering, Delhi Technological University,Delhi-110042 for providing this opportunity to carry out the present thesis work.

I would like to express my deep and sincere gratitude to my research supervisor, **Dr. A. K. Agrawal,** Department of Mechanical And Production Engineering, Delhi Technological University,Delhi-110042 for giving me the opportunity to do research and providing inspiring guidance , constructive criticism and valuable suggestion throughout this research. It was a great privilege and honour to work and study under his guidance.

Lastly my sincere thanks to all my friends, classmates , Phd scholars, Design Center staff and family who have patiently extended all sorts of help for accomplishing this undertaking.

Ishita
2K18/CDN/03

ABSTRACT

This master thesis presents research into inelastic buckling of cylindrical shells under axial loads. This type of structure is found in aerospace application like planes, launch vehicles, rockets etc. However modeling of these is not discussed here. Here the study is to see effects of plasticity on buckling loads. The idea behind this research is that in experiments we can't separate plasticity of a material but in FEA Software we can.

A FE Module is developed such that it's buckling load according to classical theory is higher than yield point. It is first analyzed with linear elastic material model and then linear elastic-nonlinear plastic, and results are compared to study effects of plasticity. Material module is developed by using nonlinear kinematic hardening equations for 2024 T3 alloy of aluminum at room temperature(25^0 C). Data points for plotting graph are found by Matlab. To find inelastic critical buckling loads an iterative method related to reduced modulus theory is tried for three different shell thickness, though it was a failure.

The results of analysis shows that there is an expected reduction of buckling load when plasticity is considered which in some cases could be about nine times of further reduction when imperfections are considered, so there is a need for a better theoretical model which would consider plasticity. The idea is maybe by studying inelastic load values we could get some insight on how to deal with theoretical equations or what kind of results should come.

CONTENTS

LIST OF FIGURES

LIST OF TABLES

LIST OF SYMBOLS AND ABBREVIATIONS

N_x , N_y, N_{xy} **and** N_{yx}	In-plane normal and shearing forces per unit edge length of a cylindrical shell element
Q_x, Q_y	Transverse shearing force per unit edge length
M_x, M_y	Bending moments
M_{xy}, M_{yx}	Twisting moments
$C = \frac{Et}{1-\mu^2}$	Coefficient used in constitutive relation, represents stiffness
$D = \frac{Et^3}{12(1-\mu^2)}$	Bending stiffness of shell
$Z = \frac{l^2}{Rt}(1-\mu^2)^{1/2}$	Batdorf factor
m	Number of half waves in longitudinal direction
n	Number of half waves in circumferential direction
$\beta = \frac{nl}{\pi R}$	where l and R are length and radius of cylinder
$\sigma_{cr} = \frac{1}{\sqrt{3(1-\mu^2)}}\frac{Et}{R}$	Critical stress for elastic buckling
$P_{cr} = \frac{2\pi}{\sqrt{3(1-\mu^2)}}Et^2$	Critical load for elastic buckling
$\rho = \frac{P_{act}}{P_{cr}}$	Knockdown factor
$\rho = 1 - 0.901(1-e^{-\phi})$	where $\phi = \frac{1}{16}\sqrt{\frac{R}{t}}$ **for** $\frac{R}{t} < 1500$
σ_e ,ε_e	Engineering stress and strain
σ, ε	True stress and strain
$\sigma^p = \frac{K}{\alpha}\left(1-e^{-\alpha\varepsilon^p}\right)$	Relation between plastic stress and strain by kinematic hardening model where $\varepsilon^p = \varepsilon - \frac{\sigma_y}{E}$ and $\sigma^p = \sigma - \sigma_y$, σ_y is yield stress
K	Kinematic hardening modulus, α is a coefficient which defines rate of decrease of K with increase of the plastic deformation.
$\sigma_{cr}\vert_p = \left(\frac{E_t E_s}{3(1-\vartheta^2)}\right)^{1/2}\frac{t}{R}$	Critical stress for plastic range, where $\vartheta = \frac{1}{2} - \left(\frac{1}{2}-\mu\right)\frac{E_s}{E}$
$E_s = \frac{\sigma}{\varepsilon}$	Secant modulus

$\boldsymbol{E_t = \frac{d\sigma}{d\varepsilon}}$	Tangent modulus
$\boldsymbol{E}$	Yong's modulus
$\boldsymbol{\mu}$	Poisson's ratio

CHAPTER 1

INTRODUCTION

1.1 Background

The phenomenon of sudden lateral bending of a slender body from its longitudinal position is called buckling. Buckling could be bifurcation type or deflection amplification type. Bifurcation buckling is a concept just to understand the phenomena and find upper bound solutions ,it is not observed in real life, even under ideal experimental conditions it is hard to occur. It basically means that load deflection curve bifurcates a lot from the prebuckling vertical graph. Till the least buckling load the load deflection curve will be straight vertical line and at buckling load theoretically there should be sudden increase in deflection making a constant function type graph passing through buckling load on vertical axis for the case of columns in case of cylinder and plates there are quadratic or cubic curves. But in real life situation there are always some imperfections present in the body and as load increases the curve won't be a vertical line (Fig.1.1).

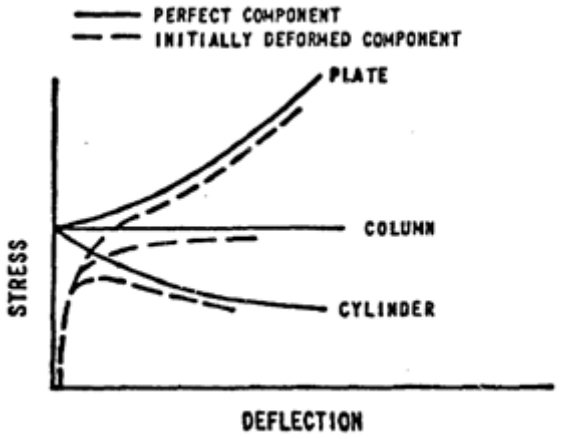

Fig. 1.1 General post buckling behavior of different types of components[13]

Slope of load curve represents stiffness of the component and negative stiffness is an indication of instability in the system (load decreases as deflection increases).Plates usually have stable ,columns neutral and cylindrical shells unstable initial postbuckling behavior Fig.1.1 .In fact one of the major design considerations in cylindrical shells is there stability

under static axial loading if loads are near buckling points very small disturbance can make structure unstable and force it to change from one equilibrium configuration to another of a different nature suddenly. In load deflection curves peak represents unstable , valleys stable and saddle points neutral equilibrium.

The classical theories refer to buckling in elastic range and do not take plasticity and yielding into account as designing is already based on strength of a material and if buckling loads are higher than yielding it already be considered. But this is not completely true as buckling of shells is highly local phenomenon and its possible that though globally structure has not buckled, locally a section it has crossed yielding stresses due to deflection if not loading. The formulas in classical theories highly overestimates the buckling loads and in real life there could be external disturbances as well. Shells have membrane stiffness which are a lot greater than bending, and if this membrane strain energy has to be released as equivalent bending stiffness energy ,the shell will deform drastically. At the locations of large deformations the stresses would cross yield value and local yielding at multiple points would start.

In practical experiments it is not possible to separate plasticity from a material. But one could do that in software. Plasticity could be studied on FEM software by taking separate elastic and inelastic material models. In one case material non linearity is ignored and then it can be compared to analysis with consideration of plasticity. There is also stress concentration due to boundary condition like clamping which could affect locations of maximum and minimum deformation.

1.2 Objective

The objectives of study presented herein are

1. To compare buckling behavior of axially loaded cylindrical shells with and without consideration of plasticity
2. To see how results from classical theory deviate from FE analysis
3. To study buckling behavior of model whose buckling load is in plastic range if calculated by classical formulas
4. To see if plasticity factor given in some literature can be used outside of its range if model has classical buckling loads in plastic range

1.3 Organization of Thesis

In chapter 2 classical theory is discussed and critical stress formula is derived by solving equilibrium equations with the help of kinematic and constitutive relations. Comparison of theoretical data with that of experiments is discussed along with causes of discrepancy.

In chapter 3 literature review for buckling theories, material modeling and inelastic buckling is given. How Abaqus can be used for buckling and postbuckling analysis is briefly discussed.

In chapter 4 FE analysis of elastic body and its comparison with classical theory is discussed. A preliminary mesh convergence study is done to choose final mesh size. Buckling behavior of perfect and imperfect shells are compared.

In chapter 5 nonlinear kinematic hardening model for plasticity is discussed for 2024 T3 aluminum alloy at room temperature. Plasticity reduction factor given in literature is discussed and finally FE analysis is done for elastic-plastic material.

In chapter 6 curves for elastic and plastic models are compared for different thickness , deformation patterns for elastic and plastic model are compared ,and possible relation between plastic loads and thickness is discussed. Buckling loads are also compared for different imperfection amplitudes.

In chapter 7 major conclusions are drawn and further study for each is recommended.

CHAPTER 2

CYLINDRICAL SHELL BUCKLING

2.1 Introduction

Shells are elements where one dimension(thickness) is very small compared to the other two. The difference between a plate element and a shell element is that the shell element has curvatures in the unloaded state. This curvature affects generalized internal forces in axial direction and moments in plane perpendicular to axis. The initial curvature does affects equilibrium equations in radial direction.

Membrane action is caused by in-plane forces. These forces may be the primary forces caused by applied edge loads or edge deformations, or they may be secondary forces resulting from flexural deformations. In a stability analysis, primary in-plane forces must be considered whether or not initial curvature exists. However, the same is not necessarily the case regarding secondary in-plane forces. If the element is initially flat, secondary in-plane forces do not affect membrane action significantly unless the bending deformations are large. It is for this reason that membrane action due to secondary forces is ignored in the small-deflection plate theory, but not in the large-deflection plate theory. If the element has initial curvature, on the other hand, membrane action caused by secondary in-plane forces will be significant regardless of the magnitude of the bending deformations. Membrane action resulting from secondary forces therefore must be accounted for in both small- and large-deflection shell theories.

2.1.1 Classical Theory

Consider a differential shell element with radius of curvature R and thickness t as shown in Fig. 2.1(a). We are using left hand Cartesian coordinates where x-axis is in axial direction, y-axis in tangential and z-axis is normal to surface and directed towards centre of curvature. The origin is in middle surface of shell.

In Fig. 2.1 (a) u, v and w are displacements in x, y and z-axis directions respectively. It

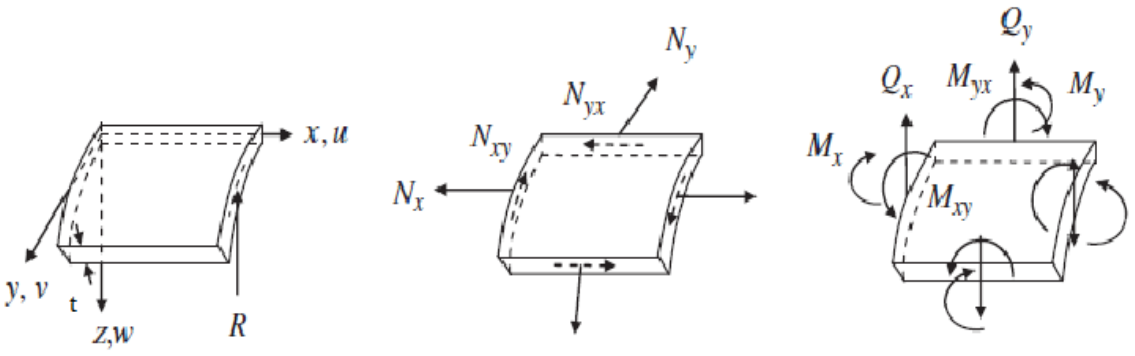

(a) (b) (c)

Fig. 2.1 Displacements and forces in cylindrical shell element

is convenient to express internal forces (generalized) per unit edge length of shell element. N_x, N_y, N_{xy} and N_{yx} in Fig.2.1 (b) are in-plane normal and shearing forces per unit edge; in Fig. 2.1(c) Q_x, Q_y are transverse shearing force per unit edge; M_x, M_y are bending moments; and M_{xy}, M_{yx} are twisting moments. The directions of moments are clearer in Fig. 2.3(b) with double arrow notation following right hand thumb rule.

They are related to internal stresses by

$$N_x = \int_{-t/2}^{t/2} \overline{\sigma_x}\left(1+\frac{z}{R}\right)dz \qquad N_y = \int_{-t/2}^{t/2} \overline{\sigma_y} dz \tag{2.1}$$

$$N_{xy} = \int_{-t/2}^{t/2} \overline{\tau_{xy}}\left(1+\frac{z}{R}\right)dz \qquad N_{yx} = \int_{-t/2}^{t/2} \overline{\tau_{yx}}\, dz$$

$$Q_x = \int_{-t/2}^{t/2} \overline{\tau_{xz}}\left(1+\frac{z}{R}\right)dz \qquad Q_y = \int_{-t/2}^{t/2} \overline{\tau_{yz}}\, dz \tag{2.2}$$

$$M_x = \int_{-t/2}^{t/2} z\overline{\sigma_x}\left(1+\frac{z}{R}\right)dz \qquad M_y = \int_{-t/2}^{t/2} z\overline{\sigma_y}\, dz \tag{2.3}$$

$$M_{xy} = \int_{-t/2}^{t/2} z\overline{\tau_{xy}}\left(1+\frac{z}{R}\right)dz \qquad M_{yx} = \int_{-t/2}^{t/2} z\overline{\tau_{yx}}\, dz$$

The stresses with bar $\overline{\sigma_x}$ or $\overline{\tau_{xy}}$ etc are that at any point through the thickness.

2.1.2 Equilibrium Equations

For nonlinear equilibrium equation we consider slightly deformed configuration like in Fig.2.3 and equate total force to zero. The angles of rotation $\frac{\partial w}{\partial x}$ and $\frac{\partial w}{\partial y}$ are assumed small ,therefore sines and cosines of them can be replaced by angles themselves and unity

respectively. Due to initial curvature of shell element the force N_y has a component in z direction (Fig.2.2).This is not the case of any other in-plane force. All the in-plane forces however have components in z direction due to curvature produced by bending Fig.2.3(a).

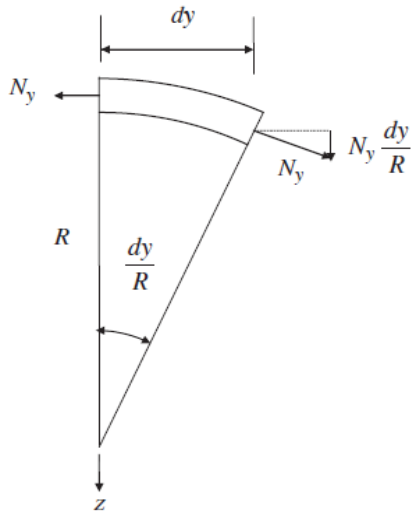

Fig.2.2 z components of in-plane forces due to initial curvature

Equating summation of forces in x and y directions equal to zero yields following equations:

$$\frac{\partial N_x}{\partial x} + \frac{\partial N_{yx}}{\partial y} = 0 \tag{2.5}$$

$$\frac{\partial N_y}{\partial y} + \frac{\partial N_{xy}}{\partial x} = 0 \tag{2.6}$$

Adding components of forces in z direction from Fig. 2.3(a) we get equation (2.7), neglecting higher order terms and regrouping we get equation (2.8). From (2.5) and (2.6) we know that values inside brackets are zero. To simplify the expression further $\frac{z}{R}$ is neglected relative to unity in (2.1), (2.2) and (2.3), then $N_{xy} = N_{yx}$ and $M_{xy} = M_{yx}$ as $\bar{\tau}_{xy} = \bar{\tau}_{yx}$ and we get equilibrium equation (2.9) in z direction. The condition that sum of moments is zero about x-axis and y-axis gives (2.10) and (2.11) respectively. Substituting values of transverse shear force from (2.10) and (2.11) in (2.9) we get (2.12).

$$-N_x dy \frac{\partial w}{\partial x} + \left(N_x + \frac{\partial N_x}{\partial x} dx\right) dy \left(\frac{\partial w}{\partial x} + \frac{\partial^2 w}{\partial x^2} dx\right)$$

$$-N_y dx \frac{\partial w}{\partial y} + \left(N_y + \frac{\partial N_y}{\partial y} dy\right) dx \left(\frac{\partial w}{\partial y} + \frac{\partial^2 w}{\partial y^2} dy\right)$$

$$-Q_x dy + \left(Q_x + \frac{\partial Q_x}{\partial x} dx\right) dy - Q_y dx + \left(Q_y + \frac{\partial Q_y}{\partial y} dy\right) dx$$

$$-N_{xy} dy \frac{\partial w}{\partial y} + \left(N_{xy} + \frac{\partial N_{xy}}{\partial x} dx\right) dy \left(\frac{\partial w}{\partial y} + \frac{\partial^2 w}{\partial x \partial y} dx\right)$$

$$-N_{yx} dx \frac{\partial w}{\partial x} + \left(N_{yx} + \frac{\partial N_{yx}}{\partial y} dy\right) dx \left(\frac{\partial w}{\partial x} + \frac{\partial^2 w}{\partial x \partial y} dy\right)$$

$$+p\, dx\, dy + N_y \frac{dy}{R} dx = 0 \qquad (2.7)$$

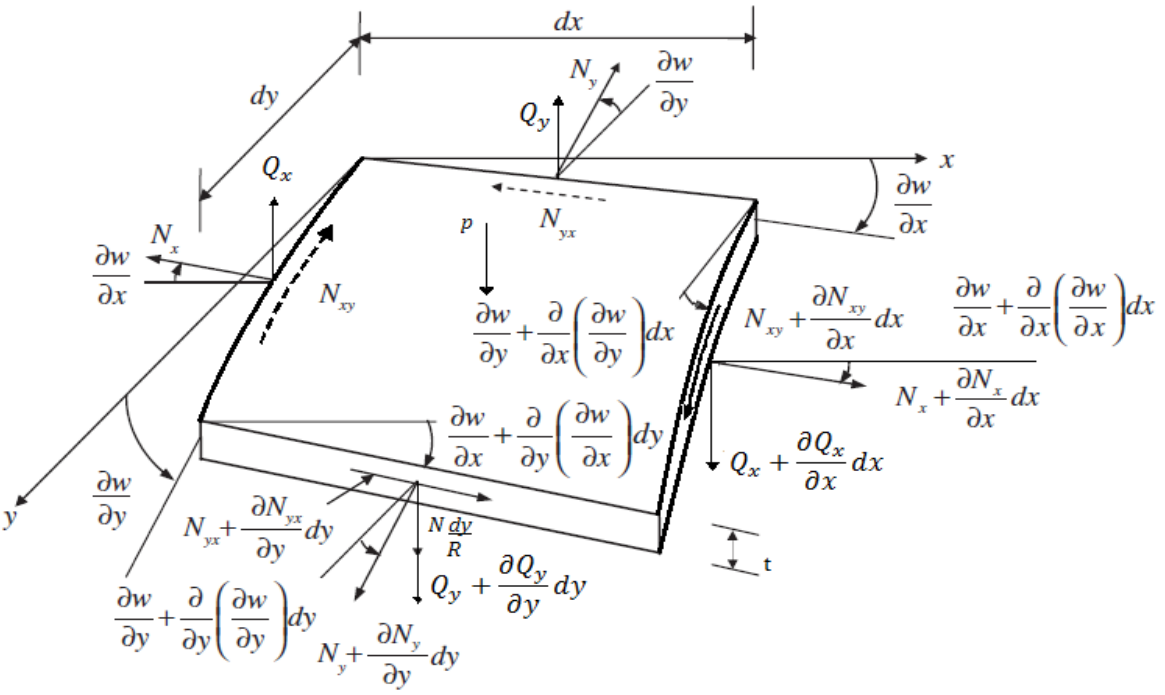

(a)

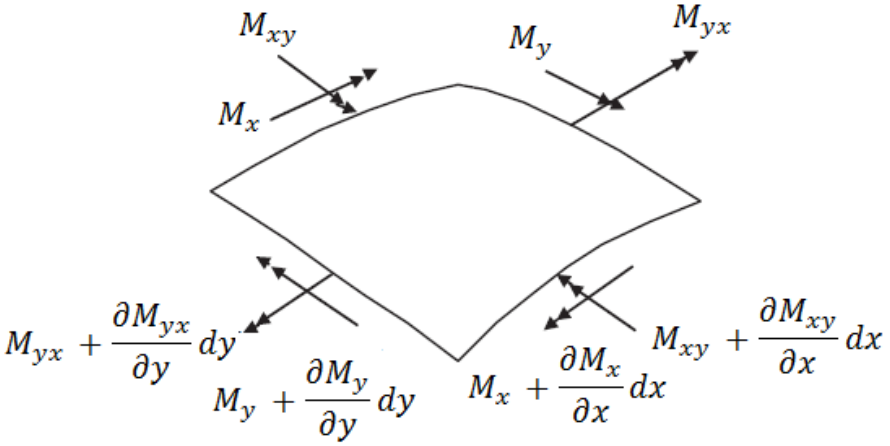

(b)

Fig. 2.3 Internal forces for slightly deformed configuration

$$\left(\frac{\partial N_x}{\partial x}+\frac{\partial N_{yx}}{\partial y}\right)\frac{\partial w}{\partial x}+\left(\frac{\partial N_y}{\partial y}+\frac{\partial N_{xy}}{\partial x}\right)\frac{\partial w}{\partial y}+N_x\frac{\partial^2 w}{\partial x^2}+N_{xy}\frac{\partial^2 w}{\partial x\partial y}+N_y\frac{\partial^2 w}{\partial y^2}+N_{yx}\frac{\partial^2 w}{\partial x\partial y}+\frac{\partial Q_x}{\partial x}+$$
$$\frac{\partial Q_y}{\partial y}+p+\frac{N_y}{R}=0 \qquad (2.8)$$

$$\frac{\partial Q_x}{\partial x}+\frac{\partial Q_y}{\partial y}+N_x\frac{\partial^2 w}{\partial x^2}+N_y\left(\frac{\partial^2 w}{\partial y^2}+\frac{1}{R}\right)+2N_{xy}\frac{\partial^2 w}{\partial x\partial y}+p=0 \qquad (2.9)$$

$$-\frac{\partial M_y}{\partial y}-\frac{\partial M_{xy}}{\partial x}+Q_y=0 \qquad (2.10)$$

$$\frac{\partial M_x}{\partial x}+\frac{\partial M_{yx}}{\partial y}-Q_x=0 \qquad (2.11)$$

$$\frac{\partial^2 M_x}{\partial x^2}+2\frac{\partial^2 M_{xy}}{\partial x\partial y}+\frac{\partial^2 M_y}{\partial y^2}+N_x\frac{\partial^2 w}{\partial x^2}+2N_{xy}\frac{\partial^2 w}{\partial x\partial y}+N_y\left(\frac{\partial^2 w}{\partial y^2}+\frac{1}{R}\right)+p=0 \qquad (2.12)$$

Therefore the nonlinear equilibrium equations for thin cylindrical shells are

$$\frac{\partial N_x}{\partial x}+\frac{\partial N_{yx}}{\partial y}=0 \qquad (2.13a)$$

$$\frac{\partial N_y}{\partial y}+\frac{\partial N_{xy}}{\partial x}=0 \qquad (2.13b)$$

$$\frac{\partial^2 M_x}{\partial x^2}+2\frac{\partial^2 M_{xy}}{\partial x\partial y}+\frac{\partial^2 M_y}{\partial y^2}+N_x\frac{\partial^2 w}{\partial x^2}+2N_{xy}\frac{\partial^2 w}{\partial x\partial y}+N_y\left(\frac{\partial^2 w}{\partial y^2}+\frac{1}{R}\right)+p=0 \qquad (2.13c)$$

2.1.3 Kinematic relations

Strains components at any point through thickness and corresponding quantities at points on mid surface are related as

$$\bar{\varepsilon_x}=\varepsilon_x+zK_x \qquad \bar{\varepsilon_y}=\varepsilon_y+zK_y \qquad \overline{\gamma_{xy}}=\gamma_{xy}+2zK_{xy} \qquad (2.14)$$

where

$$\varepsilon_x=\frac{\partial u}{\partial x}+\frac{1}{2}\left(\frac{\partial w}{\partial x}\right)^2 \qquad K_x=-\frac{\partial^2 w}{\partial x^2}$$
$$\varepsilon_y=\frac{\partial v}{\partial y}-\frac{w}{R}+\frac{1}{2}\left(\frac{\partial w}{\partial y}\right)^2 \qquad K_y=-\frac{\partial^2 w}{\partial y^2} \qquad (2.15)$$
$$\gamma_{xy}=\frac{\partial u}{\partial y}+\frac{\partial v}{\partial x}+\frac{\partial w}{\partial x}\frac{\partial w}{\partial y} \qquad K_{xy}=-\frac{\partial^2 w}{\partial x\partial y}$$

The equations above have Green Lagrange strain components ,therefore combining with equilibrium equations can be used for large deflection problems.

2.1.4 Constitutive Relations

Applying Hooke's law and bending equation to the lamina we have

$$\overline{\sigma_x} = \frac{E}{1-\mu^2}\left(\overline{\varepsilon_x} + \mu\overline{\varepsilon_y}\right) \qquad \overline{\sigma_y} = \frac{E}{1-\mu^2}\left(\overline{\varepsilon_y} + \mu\overline{\varepsilon_x}\right) \qquad \overline{\tau_{xy}} = \frac{E}{2(1+\mu)}\overline{\gamma_{xy}} \tag{2.16}$$

where E is Yong's modulus. Substituting (2.14),(2.15) and (2.16) in (2.1)and (2.3), and integrating the results gives(2.17) which are constitutive equations for thin walled isotropic elastic cylinders.

$$N_x = C\left(\varepsilon_x + \mu\varepsilon_y\right) \qquad N_y = C\left(\varepsilon_y + \mu\varepsilon_x\right) \qquad N_{xy} = C(1-\mu)\frac{\gamma_{xy}}{2} \tag{2.17}$$

$$M_x = -D\left(\frac{\partial^2 w}{\partial x^2} + \mu\frac{\partial^2 w}{\partial y^2}\right) \quad M_y = -D\left(\frac{\partial^2 w}{\partial y^2} + \mu\frac{\partial^2 w}{\partial x^2}\right) \quad M_{xy} = -D(1-\mu)\frac{\partial^2 w}{\partial x \partial y}$$

Where coefficients C and D are

$$C = \frac{Et}{1-\mu^2} \qquad D = \frac{Et^3}{12(1-\mu^2)} \tag{2.18}$$

2.2 Linearized Stability Equations

Substituting kinematic and constitutive relations for moments into equilibrium equations yields a set of three nonlinear differential equations in variables N_x, N_y, N_{xy} and w as follows

$$N_{x,x} + N_{xy,y} = 0 \tag{2.19a}$$

$$N_{xy,x} + N_{y,y} = 0 \tag{2.19b}$$

$$D\left(w_{,xxxx} + 2w_{,xxyy} + w_{,yyyy}\right) - \left[N_x w_{,xx} + 2N_{xy}w_{,xy} + N_y\left(\frac{1}{R} + w_{,yy}\right)\right] = p \tag{2.19c}$$

Linear equations can be obtained by using kinematic and constitutive relations again and dropping all the quadratic and higher order terms in u , v and w as follows

$$u_{,xx} - \frac{\mu w_{,x}}{R} + \frac{1-\mu}{2}u_{,yy} + \frac{1+\mu}{2}v_{,xy} = 0 \tag{2.20a}$$

$$\frac{1-\mu}{2}v_{,xx} + \frac{1+\mu}{2}u_{,xy} + v_{,yy} - \frac{w_{,y}}{R} = 0 \tag{2.20b}$$

$$D\nabla^4 w - \frac{C}{R}\left(v_{,y} - \frac{w_{,y}}{R} + \mu u_{,x}\right) = p \tag{2.20c}$$

First term in (2.20c)is left as that is connected to moments ,rest on LHS is related to in plane forces and RHS is related to pressure normal to surface. Here further u and v can be eliminated from (2.20c) by using operator ∇^4 as

$$\nabla^4 u = \frac{w_{,xyy}}{R} - \frac{\mu w_{,xxx}}{R} \qquad (2.21a)$$

$$\nabla^4 v = \frac{(2+\mu)}{R} w_{,xxy} + \frac{w_{,yyy}}{R} \qquad (2.21b)$$

$$D\nabla^8 w - \frac{1-\mu^2}{R^2} C w_{,xxxx} = \nabla^4 p \qquad (2.21c)$$

2.3 Application of Stability Equations to Axially Loaded Cylinders

Consider a cylindrical shell of radius R ,length l, simply supported at ends and subjected to uniformly distributed axial compressive load P.

Due to this load the cylinder shortens and except at ends its diameter increases forming an axisymmetric deformation in pre buckling range. Ideally the lateral deflection w_0 in prebuckling state should change in axial direction, here it is considered constant for sake of simplicity (Fig.2.4).

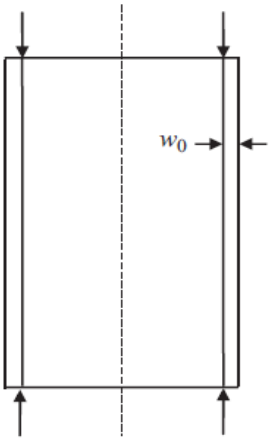

Fig.2.4 Constant lateral prebuckling deflection

For unbuckled cylinder

$$N_{x0} = -\frac{P}{2\pi R} \qquad \text{and} \qquad N_{xy0} = N_{y0} = 0$$

where subscript 0 represents pre buckled state. Substituting these in (2.21c) gives

$$D\nabla^8 w - \frac{1-\mu^2}{R^2} C w_{,xxxx} + \frac{P}{2\pi R} \nabla^4 w_{,xx} = 0 \qquad (2.22)$$

Boundary condition is $w = w_{,xx} = 0$ at x=0,l .Both differential equation and boundary conditions are satisfied if lateral displacement is of the form

$$w = a \sin\frac{m\pi x}{l} \sin\frac{n\pi y}{\pi R} = a \sin\frac{m\pi x}{l} \sin\frac{\beta\pi y}{l} \qquad (2.23)$$

where $\beta = \frac{nl}{\pi R}$, m is number of half waves in longitudinal direction and n is number of half waves in circumferential direction. Substituting (2.23) in (2.22) gives

$$D\left(\frac{\pi}{l}\right)^8 (m^2+\beta^2)^4 + \frac{Et}{R^2} m^4 \left(\frac{\pi}{l}\right)^4 - \sigma_x t \left(\frac{\pi}{l}\right)^6 m^2 (m^2+\beta^2)^2 = 0 \tag{2.24}$$

Dividing this by $D\left(\frac{\pi}{l}\right)^8$ we get

$$(m^2+\beta^2)^4 + \frac{12m^4Z^2}{\pi^4} - k_x m^2 (m^2+\beta^2)^2 = 0 \tag{2.25}$$

where

$$Z = \frac{l^2}{Rt}(1-\mu^2)^{1/2} \tag{2.26}$$

$$k_x = \frac{\sigma_x t l^2}{D\pi^2} \tag{2.27}$$

Here Z is a non dimensional variable called Batdorf parameter useful for distinguishing short and long cylinders. From (2.25)

$$k_x = \frac{\left(m^2+\beta^2\right)^2}{m^2} + \frac{12m^2Z^2}{\pi^4(m^2+\beta^2)^2} \tag{2.28}$$

Differentiating (2.28) with respect to $\frac{\left(m^2+\beta^2\right)^2}{m^2}$ and equation to zero gives condition for minimum k_x that is

$$\frac{\left(m^2+\beta^2\right)^2}{m^2} = \left(\frac{12Z^2}{\pi^4}\right)^{1/2} \tag{2.29}$$

and minimum value of k_x is

$$k_x = \frac{4\sqrt{3}}{\pi^2} Z \tag{2.30}$$

putting values of k_x and Z form (2.26) and (2.27) in (2.30) we get critical stress as

$$\sigma_{cr} = \frac{1}{\sqrt{3(1-\mu^2)}} \frac{Et}{R} \tag{2.31}$$

and corresponding buckling load as

$$P_{cr} = \frac{2\pi}{\sqrt{3(1-\mu^2)}} Et^2 \tag{2.32}$$

Equations (2.31) and (2.32) are called classical solutions for buckling of axially compressed cylinders. As there is no length term therefore load found out is for local buckling. Since *m* and *n* are positive integers (2.29) would be hard to satisfy for very short cylinders ($Z < 2.28$).Also these equations do not give correct results for Euler column buckling mode of very long cylinders(*m*=*n*=1).

Another method of deriving these equations is through the principle of potential energy.

Total potential energy is sum of strain energy of shell and loss of potential energy due to application of load. Equating first differential of potential energy gives equilibrium equations and equating second differential to zero gives stability equations.

2.4 Comparing Classical Theory with Experiments

Experiments suggest that classical theory overestimates buckling loads for intermediate to long cylinders and sometimes underestimate it for short ones. Very long slender cylinders buckle in Euler column mode .In 1960,Siede et al. published a collection of experimental results which led to the famous NASA SP-8007 guideline, published in 1965 and revised in 1968. Knockdown factor is defined as ratio of actual buckling load $\boldsymbol{P_{act}}$ to theoretical $\boldsymbol{P_{cr}}$,therefore value of one in Fig.2.5 represents theoretical buckling load, and experimental results are shown for different range of *R/t* ratio. Eqn (2.33) gives value for knockdown factor.

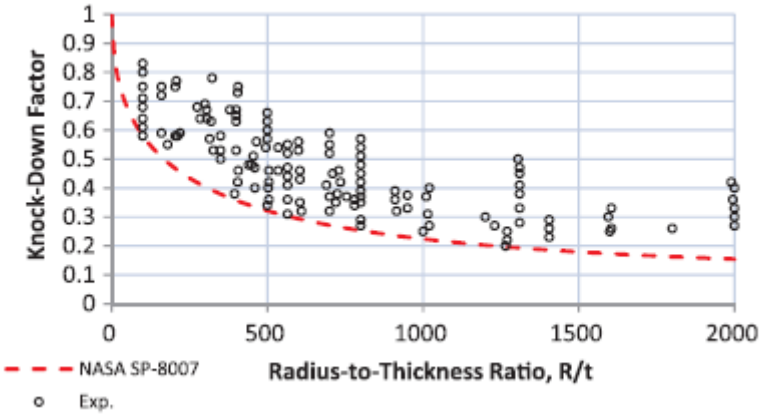

Fig.2.5 Distribution of the experimental data of axial compressed cylindrical shells for different R/t ratios from[8]

$$\rho = \frac{P_{act}}{P_{cr}}$$

$$\rho = 1 - 0.901(1 - e^{-\phi}) \tag{2.33}$$

$$\phi = \frac{1}{16}\sqrt{\frac{R}{t}} \quad \text{for } \frac{R}{t} < 1500 \tag{2.34}$$

2.5 Causes of Discrepancy Between Test and Theory

There are many factors responsible for this discrepancy like boundary conditions ,initial geometric imperfections, plasticity and residual stresses, radius and height of cylinder. Studying combination of these will tell the effects of each of them, which is now possible with computers as in experiments there is always a combination of parameters separating which is not practically possible. One such parameter is plasticity which could be easily removed or added in a software like ABAQUS as user can define material behaviour. Effect of plasticity on buckling loads is discussed in Chapter 5 and its modelling using FEM .

CHAPTER 3

LITERATURE REVIEW AND FEA IN ABAQUS

3.1 Introduction

This chapter briefly tells about the development of classical theory and how they are used now with the help of NASA guidelines. Koiter's work in the field of buckling ,post buckling and stability of elastic structures is discussed. Observations from Brushnell's design guide are stated for the plastic range and a brief overview of Maximov's material model for 2024 T3 aluminum is given.

3.2 Literature Review

Donnel[16] in 1936 , developed a large deformation theory which could develop formulations , which would take into account effect of initial geometric imperfections. He didn't measure initial deflections in tests but it was shown that most of the differences in theory and results can be explained if it is assumed that initial deflections are in the form of double harmonic series(eg-Sin A *Cos B) ,and if boundary conditions are applied buckling stress could be found as a function of yield stress, young's modulus and R/t ratio. He was the first to develop formulations which would take imperfections into account but non linear analysis failed to predict loads properly.

Karman and Tsien in 1940 showed that large discrepancies between test and theory in some shell structures is related to highly unstable post buckling behavior. Koiter[15] developed general theory for elastic stability of systems in his doctoral thesis in 1945.He developed theories in postbuckling particularly initial postbuckling and connected buckling to stability of structures. In that case second differential of total energy of the system could be used to find cases where structure is in unstable equilibrium. The theory gives asymptotes about bifurcation point ,these asymptotes represent perfect structures and as initial imperfections increases in structure the graphs would move away from these.

Although one major drawback is that this theory is not applicable outside elastic range and is limited to small magnitude of imperfections and range of validity is generally unknown.

Batdorf [17] in 1947 in his NACA(National Advisory Committee of Aeronautics) report presented modified uncoupled form of Donnel's equation for equilibrium of thin shells . There is discussion on Batdorf parameter *Z* which is related to geometry of structure. Later in 1960 Weingarten ,Seide and Morgan published a collection of experimental results which combined with Donnel's theory were base for NASA SP-8007 guideline [7] published in 1965 and revised in 1968. The guide lines basically gives knockdown factors which should be multiplied by loads calculated by classical theory (Donnel and Batdorf) to get safe load for use as one of the major drawback of classical theory is that it highly overestimates practical loads. Note Koiter's work is independent of these and it was seen that his asymptotic relations predict postbuckling behavior of different types of structures quite well.

In part four of an overview on shell buckling given by David Brushnell[11] , a rather thick aluminum cylinder under uniform axial deformation is discussed in which elastic-plastic buckle develops and at later stages it can be observed that deformations are concentrated at top end .[7] and [13] gives plasticity factors to be considered when buckling is in plastic range, but these are for a range of t/R ratios, and one could create models for materials such that buckling loads are in plastic range according to classical theory and yet does not come in this t/R range.

Maximov et al.[12] developed constitutive models for 2024-T3 aluminum alloy at room and higher temperatures in order to be used in finite element analysis of cold hole working process. The material behavior in plastic range is described by nonlinear kinematic hardening model and verified with those of uniaxial tensile test. 2024 aluminum alloy has a wide range of applications in aerospace industries for various structural shell type elements.

3.3 Using ABAQUS

In Abaqus buckling analysis is done in two steps ,first is linear perturbation to find buckling loads and modes without consideration of any nonlinearity(geometric or material). Nonlinear analysis can be further done to make load-displacement curves of the body into postbuckling regions as well, this analysis gives more robust results as non linarites are considered.

In linear eigen value analysis we look for loads which will make model stiffness matrix singular [4],thus give nontrivial displacement solutions for

$$[\boldsymbol{K}]\{\boldsymbol{v}\} = \boldsymbol{0}$$

where $\boldsymbol{K}$ is tangent stiffness matrix and $\boldsymbol{v}$ represents displacement fields. An arbitrary base configuration is considered where stresses are in equilibrium with force and traction. We consider small displacement gradient $\boldsymbol{\Delta v}$. Since problem is linear, if $\boldsymbol{K}_{\Delta}$ is differential stiffness matrix for $\boldsymbol{\Delta v}$ then it would be $\boldsymbol{\lambda K}_{\Delta}$ for $\boldsymbol{\lambda \Delta v}$ [3]. Where $\boldsymbol{\lambda}$ represents different linear perturbations to base state and among these software finds those that gives non-trivial solutions. These are called eigen values and corresponding displacement fields gives buckling modes. The iteration process is represented by following equation

$$([\boldsymbol{K_b}] + \boldsymbol{\lambda_i}[\boldsymbol{K}_{\Delta}])\{\boldsymbol{v_i}\} = \boldsymbol{0}$$

where $\boldsymbol{K_b}$is stiffness matrix corresponding to base state, $\boldsymbol{\lambda_i}$represents different linear perturbations to base state in increment $\boldsymbol{i}$.

For nonlinear analysis we have static general, static riks , dynamic implicit and dynamic explicit steps available in abaqus to plot load-deflection curve of the whole structure and check its stiffness variation. The element used (S8R5-good for analysis of shell application[5]) is not available for explicit analysis and riks method which used arc length method is the most convenient among the rest, as it calculates load proportionality factor which can be multiplied by applied load(could be any value) to get variation of load during analysis history, unlike static general and dynamic implicit which uses newton raphson method. To draw load-displacement curves in newton method steps one has to find reaction at all the end nodes and add it to get total reaction force and applied load should be greater than least buckling load.

CHAPTER 4

VARIFICATION OF ELASTIC BUCKLING THEORY USING FEM

4.1 Introduction

In this chapter ABAQUS 6.14 is used for finite element analysis. In ABAQUS buckling analysis is done in two steps ,linear perturbation analysis and nonlinear analysis. Linear perturbation analysis is used to get buckling loads and modes for a perfect cylinder ,these values can be compared to that given by Eqn (2.31).Then nonlinear analysis is done first for perfect body then for imperfect body taking first twenty eigen mode combination as imperfection, and imperfection amplitudes as 1%,10%and 20% of shell thickness . Lower range of this result is taken from NASA SP-8007 guideline[7] by calculating knockdown factors for relevant R/t ratio.

4.2 Linear perturbation of perfect cylinder

A perfect thin cylindrical shell of radius 100 *mm* ,length 200 *mm* and thickness of 1 *mm* is used. Aluminum alloy 2024 T3 is used with elastic modulus 68563 *MPa* (25^0 C)and poison's ratio .33 .As Batdorf factor is 3775.92 equation (2.32) can be used .The buckling load according to classical theory is 263.48 KN . The cylinder is modeled with eight noded doubly curved shell element S8R5 having five degrees of freedom at each node and recommended for thin shell applications [5]. Boundary conditions are applied to the reference points tied to all the end nodes through rigid body tie constraint for convenience. Boundary condition is that all degrees of freedom of end nodes are restrained except for axial movement of top nodes. Lanczos solver is used to calculate twenty buckling modes which could later be used to seed imperfection. Mesh sensitivity study is carried out by comparing eigen values and mode shapes.

4.2.1 Mesh Sensitivity Study

Global mesh sizes of 10mm,5mm,4mm,and 3mm are used for mesh sensitivity study. The results are shown in Table 4.1 .

A mesh size of 5mm is for the first time giving value nearer to converging value and there is difference of about 100s in cpu time from 10mm.Later convergence is checked for 4mm and 3mm and cpu time is increasing in each mesh by about 50s. The 4mm mesh is having convergence to first decimal value as loads are in KN this should be considered but 3mm mesh will take up too much time in nonlinear analysis .So considering cpu time and converging load value it is decided to use a 4mm mesh for the analysis.

The buckling mode shape (number of longitudinal half waves *m,* and circumferential half waves *n*)for all meshes at first eigen value is same. Note that 3.* in the values of *m* means there are more than three half waves but are not fully developed at ends due to clamped boundary condition. The results of linear perturbation analysis shows that classical theory overestimates the results for this case.

Table 4.1 Results of mesh convergence

Mesh Size	**10mm**	**5mm**	**4mm**	**3mm**
CPU Time(s)	37.3	145.6	237.3	306.6
Mode	**Buckling load(KN)**			
First mode(m,n)	3.*,18	3.*,18	3.*,18	3.*,18
1	260.75	259.60	259.54	259.51
2	260.75	259.60	259.54	259.51
3	260.77	259.62	259.56	259.53
4	260.77	259.62	259.56	259.53
5	263.00	262.10	262.05	262.02
6	263.00	262.10	262.05	262.02
%error	1.03	1.45	1.49	1.5

3.* means there are 3 full half waves but some partial half waves too

4.3 Perfect Cylinder

Nonlinear(geometric nonlinearity is considered) analysis with static riks step is used to plot load vs end displacement curves for a perfect shell(without any initial geometric imperfections). The graph is drawn into postbuckling region to study stability of the body under axial load. It is seen that thought linear perturbation solution was converging to a value lower than classical theory ,in when geometric nonlinearities are considered for a

perfect shell there is a change in stiffness of the body at about 220MPa load (Fig. 4.1) but structure is still stable and at 263.2MPa it loses its stability, which is quite close to buckling load given by classical theory. This is probably due to the reason that in linear

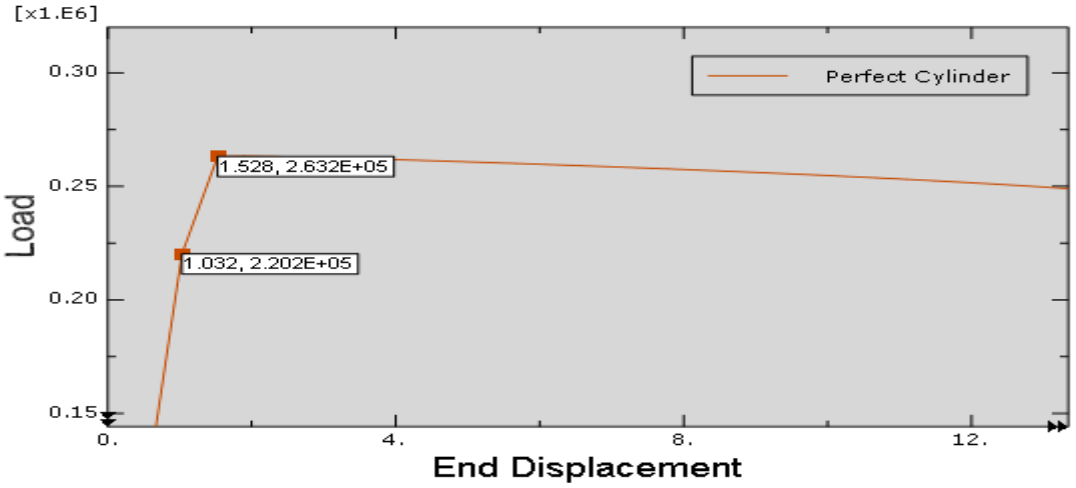

Fig. 4.1 Curve for perfect cylinder near buckling point

perturbation step any type of nonlinearity is ignored even geometric and classical theory considers finite deformations.

4.4 Effect of Imperfection

All real bodies have some imperfections in shells these could be due to some surface scratch or dent, irregularities due to rolling and other manufacturing processes etc. Curves changes due to these imperfections and buckling loads can decreases by as much as seventy percent of that calculated by classical theory. Koiter[15] theorized that one could take perfect body graphs as asymptotes for the imperfect graphs, the equations that he derived gave results quite similar to those found through experiments.

NASA SP-8007 guideline[7] gives lower bound for the imperfect shells for different r/t ratios as explained in section 2.4 and equation (2.33) is used to find knockdown factor which came out to be .5812 and the corresponding lower bound load is 153.15MPa. First twenty eigen modes from the linear analysis are used to seed imperfections ,these modes are shown in Table 4.2 . Plots for all the imperfections and prefect body are shown in Fig. 4.2 for comparison among each other. For imperfections of amplitudes 10% and 20% of the thickness , the shells started buckling below SP-8007 limits, but that could be explained through the fact that practically initial deflections are less than 10% to not be seen by eyes

or rejected during some quality test(Fig. 4.3) and the guide line is made for those shells which would be used in various applications. Here such high values are taken only to

Table 4.2 Eigen modes used to seed imperfection

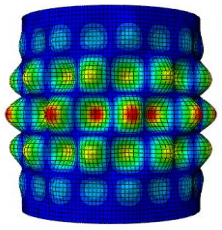	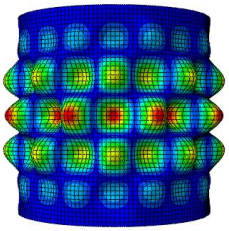	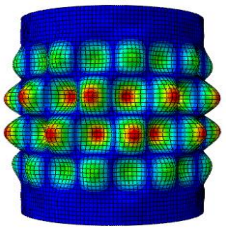	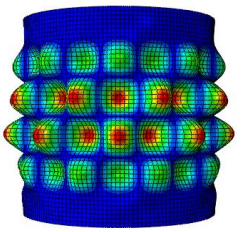
259.54MPa	249.54Mpa	259.56MPa	259.56MPa
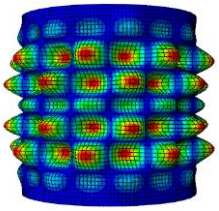	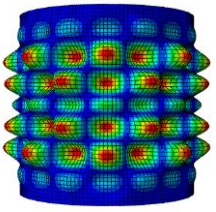	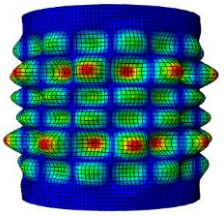	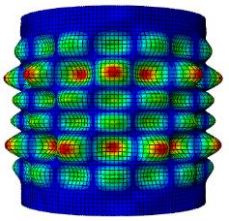
262.05MPa	262.05MPa	262.08MPa	262.08MPa
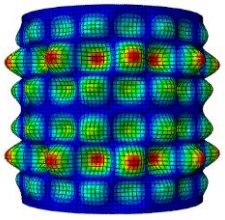	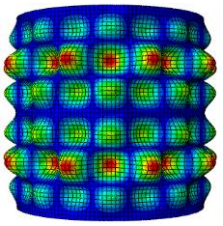	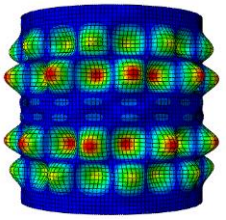	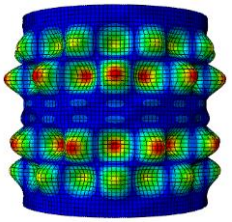
262.61MPa	262.61MPa	263.14MPa	263.14MPa
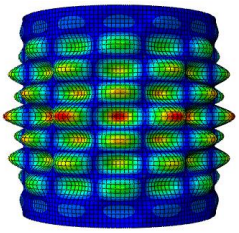	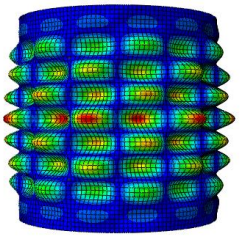	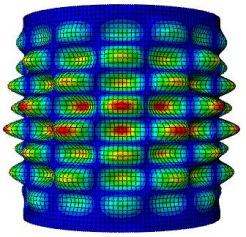	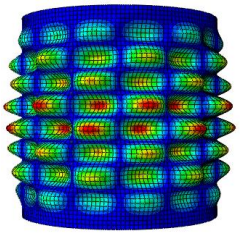
263.47MPa	263.47MPa	263.55MPa	263.55MPa
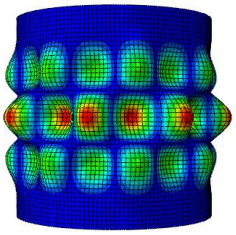	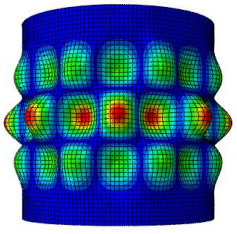	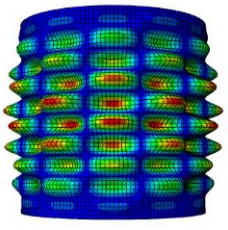	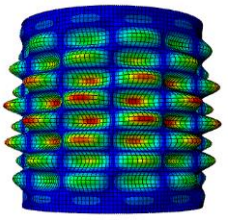
264.28MPa	264.28MPa	264.35MPa	264.35MPa

amplify deflection patterns and study them. In Fig. 4.39(a) the shell looks perfect but has

1% initial geometric deformation in the shape of first twenty eigen modes. These figures are not scaled ,this is what it would look like in real life. It could be seen from the results that graphs for imperfect bodies are asymptotic to that for perfect body supporting Koiter's

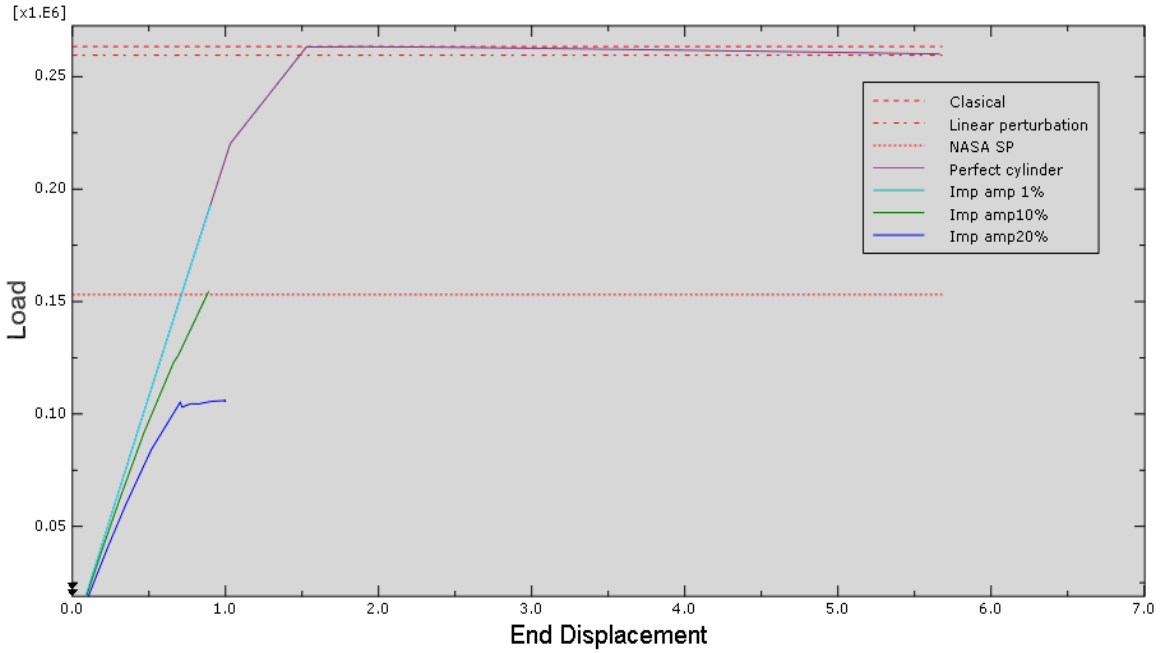

Fig. 4.2 Plot of elastic model for different imperfection amplitudes

theory. In fact curve for imperfection amplitude of 1% of thickness looks almost coinciding with perfect curve ,though there is some gap just can't be seen at this scale.

One more observation could be that, from riks step on perfect body the mode of deformation formed is not similar to that of least eigen mode of linear perturbation but higher one, infact it is similar to eigen mode corresponding to load of 163.14MPa which in turn is near to that by classical theory. So in abaqus final buckling load should be decided by combining linear perturbation (for loads) and riks method(for expected mode shape).

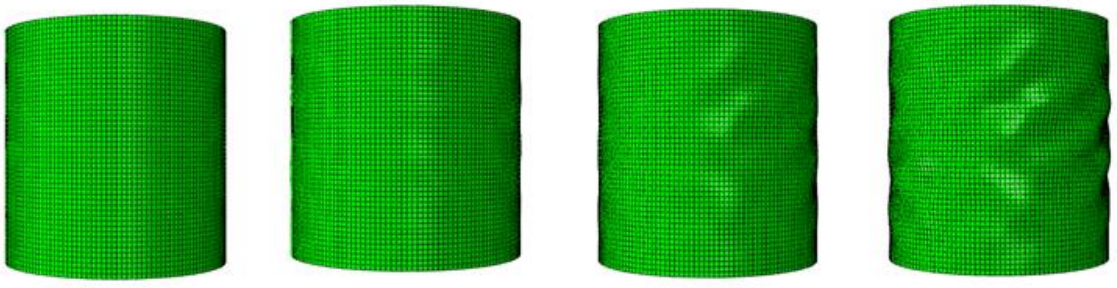

(a)1% (b)10% (c)20% (d)50%

Fig. 4.3 Initial geometric imperfections on undeformed body for different imperfection amplitudes

CHAPTER 5

INELASTIC BUCKLING AND MATERIAL MODELING

5.1 Introduction

An approximate solutions for inelastic buckling loads for axial compressions case is given in [7], [9] and [13] for radius to thickness ratios such that there is chance of buckling to go into plastic range but shell is thin at the same time. In [13] the given range is $10<\frac{R}{t}<50$,although one of the ratios taken in this study is not in this range(R=100mm and t=1 mm as in last chapter),even that is taken in a way that buckling stress falls between yielding and ultimate stresses for our material(2024 T3 Al) in uniaxial tensile test[9]. Nonlinear kinematic hardening model is used to draw true stress strain curve at room temperature with values taken from [12].

5.2 Material Model

In elastic region linear behavior is considered and for plastic region a nonlinear kinematic hardening model is presented in [12] for 2024 T3 Al at different temperatures. For this analysis data is taken corresponding to room temperature (25^0 C) and equations are written in a simplified form. Let $\boldsymbol{\sigma_e}$ and $\boldsymbol{\varepsilon_e}$ represent engineering stress and strain which is found by experiments ,then expressions for true stress ,strain ($\boldsymbol{\sigma}$, $\boldsymbol{\varepsilon}$) are

$$\sigma = \sigma_e(1+\varepsilon_e) \qquad \varepsilon = ln(1+\varepsilon_e) \tag{5.1}$$

In plastic range equivalent plastic strain is given by

$$\varepsilon^p = \varepsilon - \frac{\sigma_y}{E} \tag{5.2}$$

where σ_y is true yield stress and E is Yong's modulus. Similarly a term σ^p is defined as

$$\sigma^p = \sigma - \sigma_y \tag{5.3}$$

and from kinematic hardening model it's value is given as

$$\sigma^p = \frac{K}{\alpha}\left(1 - e^{-\alpha\varepsilon^p}\right) \tag{5.4}$$

where K is kinematic hardening modulus, $\alpha$is a coefficient which defines rate of decrease

of K with increase of the plastic deformation. Values of σ_y , K and E at various temperatures with $\alpha = 10$ are given in [12].For this analysis these values at 25^0 C are

$$\sigma_y = 369.47MPa \qquad K = 2447.66MPa \qquad E = 68563MPa$$

The stress strain plot is shown in Fig.5.1.

5.3 Inelastic Buckling

Very long slender cylinders buckle in Euler column mode and rest in a more localized axisymmetric(bellows) or asymmetric(diamond pattern).For intermediate length cylinders we find buckling loads for both type of modes and take the lower one as solution. A simple

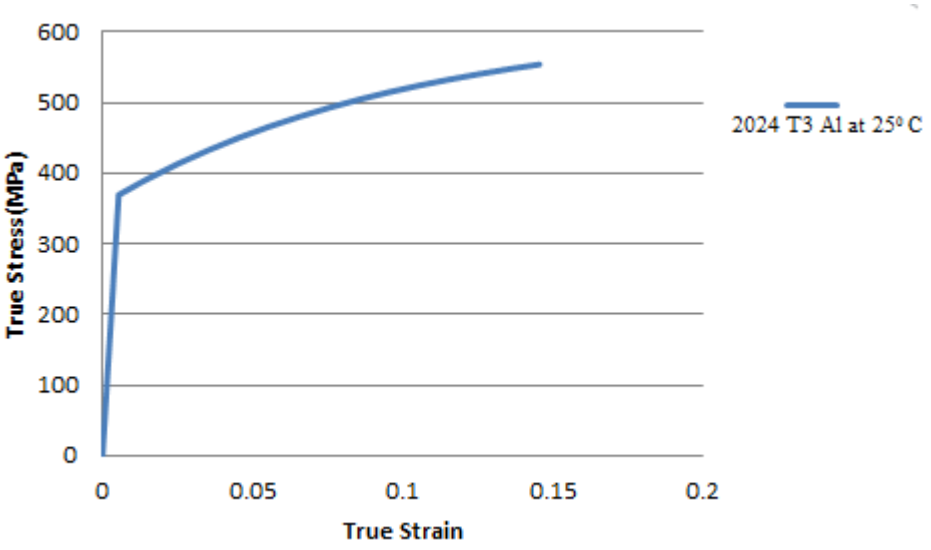

Fig. 5.1 Material model for 2024 T3 Al

solution is provided in [13] to find inelastic loads for localized buckling modes as

$$\sigma_{cr}|_p = \left(\frac{E_t E_s}{3(1-\vartheta^2)}\right)^{1/2} \frac{t}{R} \tag{5.5}$$

where $$E_s = \frac{\sigma}{\varepsilon} \qquad E_t = \frac{d\sigma}{d\varepsilon}$$

$$\vartheta = \frac{1}{2} - \left(\frac{1}{2} - \mu\right)\frac{E_s}{E}$$

E is Yong's modulus and μ is Poisson's ratio. Note E_s and E_t are secant and tangent modulus respectively, and are changing with stress, strain values on $\sigma - \varepsilon$ curve ,therefore the solution of (5.5) is an iterative process. Let P be an assumed axial load then stress corresponding to it for pure axial compression will be $\sigma_a = \frac{P}{2\pi Rt}$, E_s and E_t are found corresponding to σ_a from $\sigma - \varepsilon$ curve , σ_{cr} is calculated with these values and compared

with assumed value σ_a ,if they are same it is the solution if not another axial load is assumed till we get a solution. To find solution in this case data points on stress-strain

Table 5.1 Iterative Solution for Buckling Loads in Plastic Range

$\boldsymbol{\varepsilon}$	$\boldsymbol{\sigma}$ (MPa)	$\boldsymbol{E_s = \frac{\sigma}{\varepsilon}}$ (MPa)	$\boldsymbol{E_t = \frac{d\sigma}{d\varepsilon}}$ (MPa)	$\boldsymbol{\sigma_{cr}}$ (MPa) t=1	$\boldsymbol{\sigma_{cr}}$ (MPa) t=2	$\boldsymbol{\sigma_{cr}}$ (MPa) t=3
0	0	68563(E)	68563(E)	419.33	838.68	1258.02
0.005388(ε_y)	369.47	68572.75	2447.7	79.2368	158.4736	237.7104
0.0054	369.47	68420.37	2214.7	75.298	150.596	225.894
0.0154	392.7626	25504.06	2004	45.8833	91.7666	137.6499
0.0254	413.8385	16292.85	1813.3	35.3345	70.669	106.0035
0.0354	432.9089	12229.06	1640.7	29.2934	58.5868	87.8802
0.0454	450.1644	9915.515	1484.6	25.1789	50.3578	75.5367
0.0554	465.7779	8407.543	1343.3	22.1054	44.2108	66.3162
0.0654	479.9056	7338.006	1215.5	19.6772	39.3544	59.0316
0.0754	492.6888	6534.334	1099.8	17.6848	35.3696	53.0544
0.0854	504.2555	5904.631	995.1	16.0067	32.0134	48.0201
0.0954	514.7216	5395.405	900.4	14.5663	29.1326	43.6989
0.1054	524.1916	4973.355	814.8	13.3125	26.625	39.9375
0.1154	532.7605	4616.642	737.2	12.2071	24.4142	36.6213
0.1254	540.5139	4310.318	667.1	11.2258	22.4516	33.6774
0.1354	547.5295	4043.792	603.6	10.3472	20.6944	31.0416
0.1454	553.8774	3809.336	2447.7	20.2311	40.4622	60.6933

curve plotted in material modeling is taken as assumed values and critical stresses according to (5.5) were found for 1mm,2mm ,and3mm shell. It was found that not just this doesn't give a solution the critical stresses found were absurd Table 5.1for all three thicknesses. As critical stress is directly proportional to thickness ,as we increase thickness we will get in the range where this methods give some results (about 5mm and above) but 2mm is at boundary and 3mm is clearly within the given range yet no results[13].

CHAPTER 6

RESULTS AND DISCUSSION

6.1 Introduction

Same model as in chapter 4 is used with two more models of thickness 2mm and 3mm(other dimensions same) and fifteen equally spaced points are used to input plastic behavior in ABAQUS for accurate analysis (Table 5.1).From classical theory the buckling load is 263.47kN, 1053.91kN and 2371.3kN for shells of thickness 1mm,2mm,3mm respectively. Nonlinear(geometric nonlinearity is considered) analysis with static riks step is used to plot load vs end displacement curves for a perfect shell(without any initial geometric imperfections) with(inelastic) and without(elastic) consideration of material nonlinearity in plastic range. Later same is done for 1mm thick shell with imperfection sizes of 1% and 10% of thickness.

6.2 Perfect Materially Nonlinear Body

Here perfect means without any initial geometric imperfection. If we multiply yield stress(318.3MPa) with cross-section area we get 199.9kN,399.9kN and 599.98kN yielding loads corresponding to shell thickness of 1mm,2mm and 3mm respectively. From FEA we get plastic loads 198.6kN ,444.8kN and 682.9kN for the three thicknesses(Fig. 6.1). It is observed that even though classical theory gives buckling load above yield point FEA shows them to be within elastic limit 318.3MPa for 1mm thickness when linear elastic ,nonlinear plastic model is considered. Loads are above yielding loads for 2mm and 3mm shell.

In Fig.6.2 deformation pattern for perfect elastic and inelastic shell is compared. It can be observed that when plasticity is considered deformations starts at ends where as it is in mid length when material nonlinearity is not considered. If we further compare it with Fig.6.3 which shows a thick aluminum cylinder buckling into plastic range from an experiment, we can observe this similarity, though it was not pointed out in relation to plasticity by author[11].It could be reasoned that due to clamping there is stress concentration near ends. The material would cross yielding limit at points near ends earlier

than at those further away or near mid length.

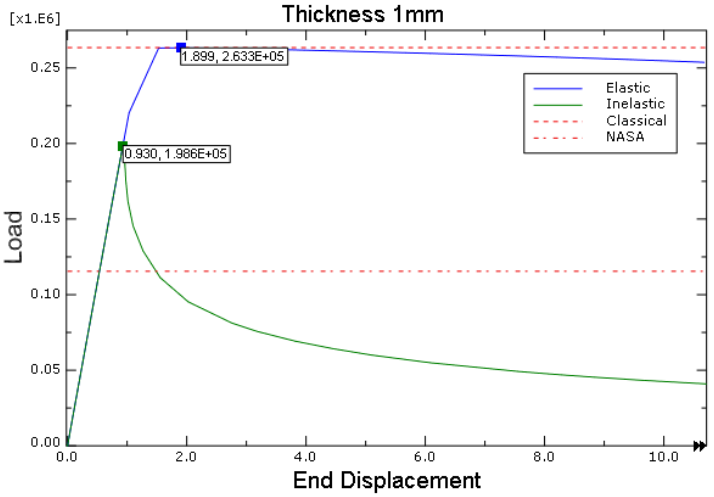

(a)

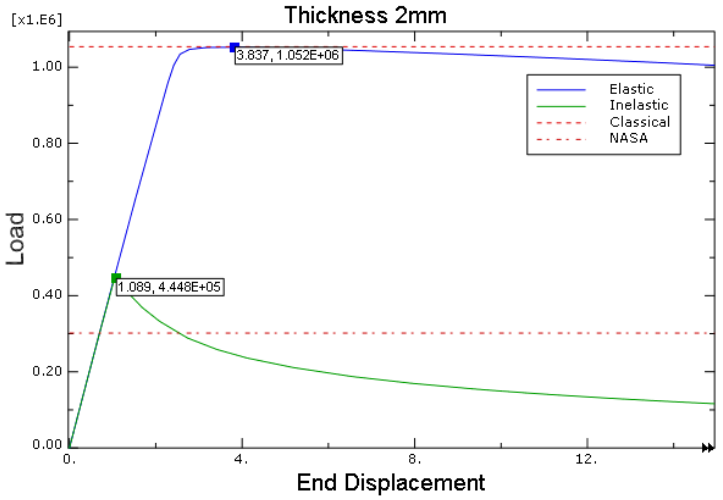

(b)

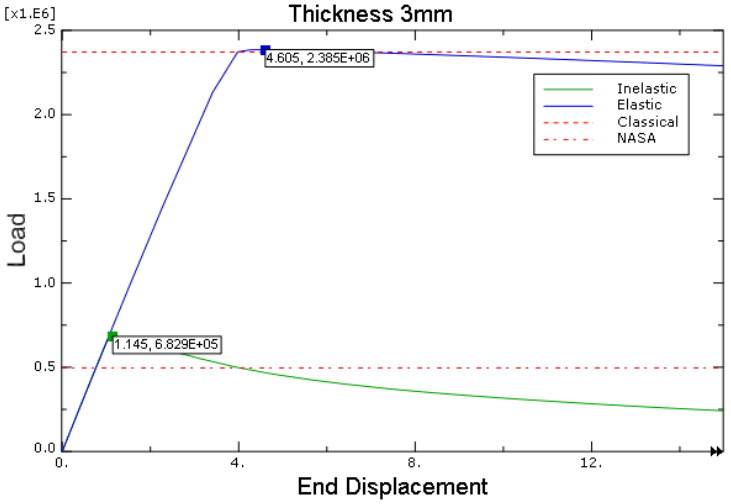

(c)

Fig. 6.1 Comparison of elastic and inelastic buckling for perfect shell of various thickness

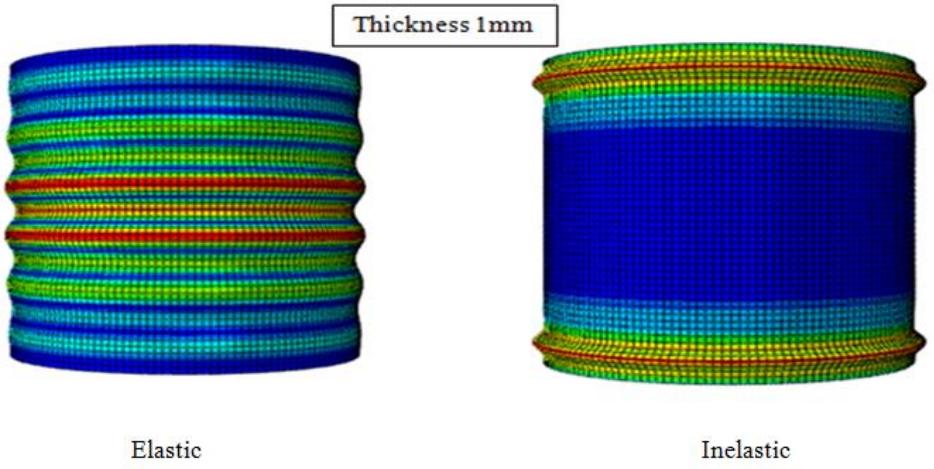

Fig. 6.2 Comparison of elastic and inelastic deformation pattern for perfect cylinder

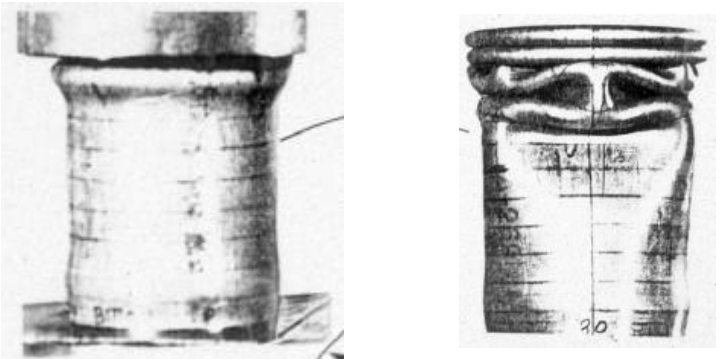

Fig. 6.3 Thick aluminum cylinder under uniform axial compression[11]

Table 6.1 Comparison of Elastic and Inelastic Buckling Loads for perfect shells

Thickness	Elastic load(Pe) in kN	Inelastic Load(Pi) in kN
1mm	263.478	198.597
2mm	1053.915	444.839
3mm	2371.310	682.931

From (2.32) if material, radius and length is same and let P_e denote elastic load and P_{e1} ,P_{e2} … represent elastic load for t_1,t_2…. shell thickness respectively then

$$\frac{P_{e1}}{P_{e2}} = \left(\frac{t_1}{t_2}\right)^2 \tag{6.1}$$

Now let t_1=1mm ,t_2 =2mm and t_3 =3mm and P_{i1} ,P_{i2}….represents inelastic loads .It could be seen from Table. 6.1, that inelastic loads don't follow relation (6.1) in fact data follows more of an arithmetic progression with respect to thickness. On the other hand if one takes difference between elastic and inelastic buckling loads for each value of thickness one might find a relation like (6.1) for different power. This study could be further extended

with more data values to find some correlation.

6.3 Analysis with Imperfections

Load vs end displacement curves are compared for 1% and 10% imperfection magnitude with perfect model, classical theory(elastic), and SP-8007 lower bound for 1mm thick model. From Fig. 6.4 it can be observed that just by consideration of plastic data(for perfect shell) buckling load is reduced by 68.5kN. It would further reduce when imperfections are considered.

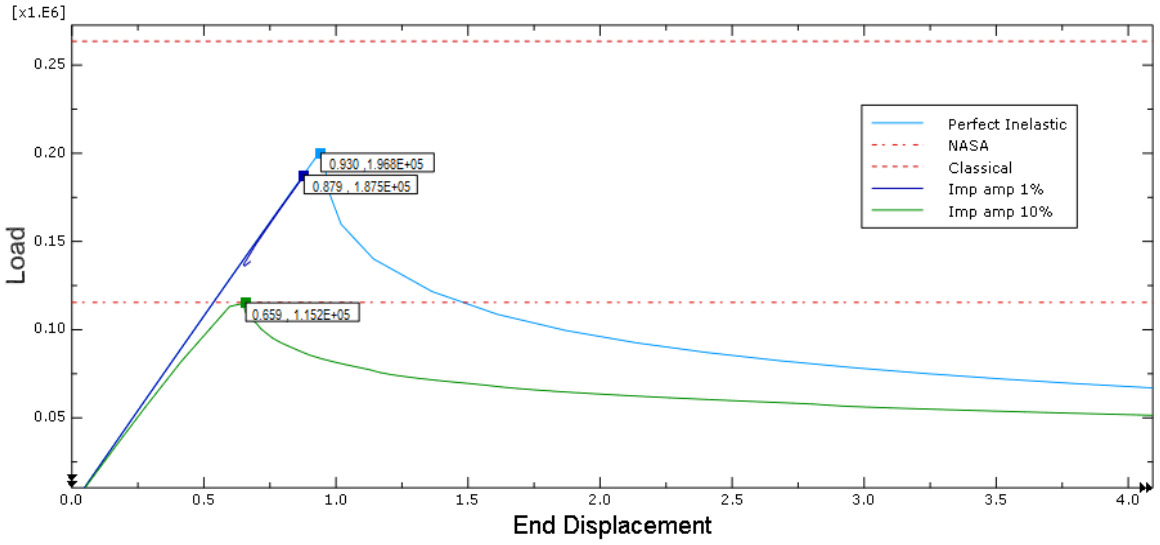

Fig. 6.4 Comparison of inelastic buckling for different imperfection amplitude for 1mm thick shell

It can also be seen that for imperfection amplitude of .01mm(1% thickness) buckling load is further decreased by 7.479kN. It is quite clear that major decrease in buckling load from classical theory is due to plasticity rather than imperfections in this case. One could argue about imperfect shells with 10% imperfection amplitude should not be below nasa lower bound but that is quite high imperfection amplitude taken just to get some smooth curve to see postbuckling behaviour.

CHAPTER 7

CONCLUSION AND RECOMENDATIONS

1-There is a change in location of maximum lateral deformation from mid length to ends for perfect cylinders without and with plasticity considerations respectively. It is recommended to study deformation patterns for different end conditions.

2-There was a case where drop in buckling load by consideration of plasticity for perfect body is higher than further drop due to imperfection. It is recommended to use this method of analysis for a lot of different material and geometric model combinations.

3-Thouth SP-8007 knockdowns are valid the study indicate that a range of different values for same R/t ratio could be due to different material properties as well(elastic modulus of material doesn't affect knockdown factor as it is cancelled out eqn(2) but yield points could affect experimental output) other than random initial imperfections. This means following that guideline one could be designing over safe structures with extra material mass and this type of study might help us save material cost.

4-Ratio of elastic buckling loads is proportional to square of respective shell thickness if material and rest of the geometry is unchanged. Same is not true for inelastic loads , in fact they show somewhat an arithmetic progression patterns and difference in elastic and inelastic loads shows a higher order pattern. It is recommended to collect a lot more data to study it further for some correlation if any, it might give some insight for theoretical study.

REFERENCES

[1] Timoshenko, S. P., and J. M. Gere, *Theory of Elastic Stability,* 2nd Edition, McGraw-Hill, New York, 1961.

[2] Chai H. Yoo and Sung C. Lee ,*Stability of Structures-Principles and Applications,* 2011, Elsevier Publication

[3] Dassault Systemes Simulia Corp. Abaqus 6.14,*Abaqus Theory Guide*

[4] Dassault Systemes Simulia Corp. Abaqus 6.14,*Abaqus Analysis User's Manual*

[5] Dassault Systemes Simulia Corp. Abaqus 6.14,*Abaqus Benchmarks Guide*

[6] Dassault Systemes Simulia Corp. Abaqus 6.14, *Abaqus Example Problems Guide*

[7] Peterson J.P., Seide P., and Weingarten V.I., *Buckling of thin-walled circular cylinders.* Technical Report NASA SP-8007, 1968.

[8] H.N.R. Wagner, C. Huhne, S. Niemann and R. Khakimova ,*Robust Design Criterion for Axially Loaded Shells-Simulation and Validation,* Thin-Walled Structures 115(2017)154-167

[9] G.Gerard and H.Becker , *Buckling of Curved Plates and Shells,* Handbook of Structural Stability Part III ,NACA TN 3738,1957

[10] Fan Ye, Delft University of Technology, Master Thesis , *Local Buckling Analysis of Thin-Wall Shell Structures,*2015_10_2

[11] David Bushnell , *Buckling of Shells Pitfall for Designers*. AIAA Journal, 19(9):1183– 1226, 1981.

[12] J.T.Maximov et al. ,*Modeling of Strain Hardening and Creep Behavior of 2024T3 Aluminium Alloy at Room and High Temperatures,*Computational Materials Science 83 (2014) 381-393

[13] D.S.Griffin ,*Inelastic And Creep Buckling of Circular Cylinders due to Axial Compression,Bending, and Twisting* 1973

[14] Dassault Systemes Simulia Corp. Abaqus 6.14,*Getting Started with Abaqus/CAE*

[15] J.W. Hutchinson ,W.T. Koiter ,*Postbuckling Theory,* Applied Mechanics Review,1970

[16] L.H. Donnel, Akron OHIO,*A New Theory for Buckling of Thin Cylinders*

Under Axial Compression and Bending, ASME ,Vol. 56, 795-806

[17] S.B. Batdorf ,*A Simplified Method of Elastic-Stability Analysis for Thin Cylindrical shells,* NACA Report No. 874,1947

[18] B.O. Almroth ,A.M.C. Holmes and D.O. Brush, *An Experimental Study of the Buckling of Cylinders Under Axial Compression,* September 1964

[19] Bernard Budiansky, *Theory of Buckling and Postbuckling Behaviour of Elastic Structure* ,Advances in Applied Mechanics -1974

LIST OF PUBLICATIONS

1- Ishita, *Effect of Inelasticity on Buckling of Axially Compressed Cylindrical Shell*, Submission 330, EMSME 2020 conference, accepted with a score of 3(strong acceptance)

EMSME 2020 notification for paper 330 and Registration Details Inbox x

EMSME 2020 <emsme2020@easychair.org> Sep 25, 2020, 3:16 PM

to me

Dear Authors,

I am pleased to inform you that your submission to EMSME-2020 has been accepted for consideration for publication in LNEE/ LNME, a Scopus indexed, Springer publication.

Please find below the comments of the reviewers for your considerations.

SUBMISSION: 330
TITLE: Effect of Inelasticity on Buckling of Axially Compressed Cylindrical Shell

---------- REVIEW 1 ----------
SUBMISSION: 330
TITLE: Effect of Inelasticity on Buckling of Axially Compressed Cylindrical Shell
AUTHORS: Ishita

---------- Overall evaluation ----------
SCORE: 3 (strong accept)

Abstract:

Effect of Inelasticity on Buckling of Axially Compressed Cylindrical Shell

Ishita[1][0000-1111-2222-3333]

[1] Delhi Technological University, Shahbad Daulatpur village,Rohini,Delhi 110042

Abstract. The idea behind this research is that in experiments we can't separate plasticity of a material but in FEA Software we can. FE models are developed such that their buckling load according to classical theory are higher than yield point. It is first analysed with linear elastic material model and then linear elastic-nonlinear plastic, and results are compared to study effects of plasticity. Material model is developed by using nonlinear kinematic hardening equations for 2024 T3 alloy of aluminum at room temperature(25^0 C). To find inelastic critical buckling loads an iterative method related to reduced modulus theory is tried for three different shell thickness, though it was a failure. The results of analysis shows that there is an expected reduction of buckling load when plasticity is considered which in some cases could be about nine times of further reduction when imperfections are considered, so there is a need for a better theoretical model which would consider plasticity. The idea is maybe by studying inelastic load values we could get some insight on how to deal with theoretical equations or what kind of results should come.

Keywords: Buckling, Inelastic, Finite Element Analysis.